Available online at www.sciencedirect.com

ScienceDirect

Mendeleev Commun., 2022, **32**, 327–330

Mendeleev Communications

High performance carbon–carbon composites obtained by a two-step process from phthalonitrile matrix composites

Vladislav V. Aleshkevich,*[a] Boris A. Bulgakov,[a,b] Yakov V. Lipatov,[a] Aleksandr V. Babkin[a,b] and Alexey V. Kepman[a,b]

[a] *Department of Chemistry, M. V. Lomonosov Moscow State University, 119991 Moscow, Russian Federation. E-mail: vladislav.aleshkevich@gmail.com*

[b] *Institute of New Carbon Materials and Technology, 119991 Moscow, Russian Federation*

DOI: 10.1016/j.mencom.2022.05.011

Carbon–carbon composites (C/C) were produced from carbon fiber reinforced phthalonitrile (CFRP) matrix composites in a two-step impregnation–carbonization procedure. After graphitization at 1800 °C, the obtained C/C composites demonstrated highly crystalline structure and properties characteristic of composites derived from phenolic matrix CFRP by the industrial procedure: d = 1.73 g cm^{-3}, interlaminar shear strength was 14.1 MPa, compression strength was 139.8 MPa, and coefficient of friction was in the range 0.32–0.34.

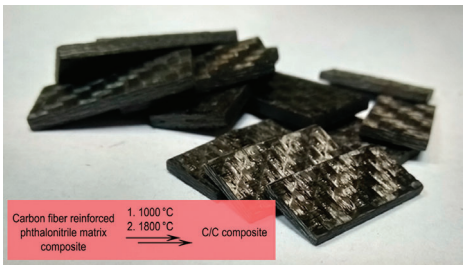

Keywords: carbon–carbon composite, C/C composites, phthalonitrile, carbonization, graphitization, vacuum infusion.

Carbon–carbon composites are a unique class of materials that can be used for applications at temperatures up to 3000 °C not only without a drop in the mechanical strength, but even with a slight enhancement after 600 °C.[1] This property determines the high demand for C/C composites in the aerospace industry and heavy vehicle manufacturing inasmuch as materials with high heat resistance are essential[2–4] for applications in brake systems,[5–8] chemical industrial equipment for high-temperature operations,[9] *etc*. The main drawback of C/C composites is their long production cycle including multiple carbonization–impregnation stages.[9–12] The finishing graphitization is also required since the highly oriented graphite matrix is more thermally stable[13] and shows higher friction and wear performance. Phenolic resins are the most widely used sources of carbon in the manufacturing of C/C composites from carbon fiber reinforced phthalonitrile (CFRP) matrix composites owing to their relatively low price and good performance.[14] On the other hand, the mass loss during carbonization (33–45%), featured to phenolics, causes a large number of cracks and voids to form in the resulting material.[15] Phthalonitrile matrices might be an alternative to phenolic resins as a carbon source in C/C fabrication by carbonization of CFRP due to their high char yield and processing requirements suitable for cost-effective injection-based CFRP fabrication methods.[16–22] The first efforts to employ phthalonitriles in the production of C/C composites have been reported recently.[23,24]

In this work, C/C composites were manufactured from CFRP (see details in Online Supplementary Materials) in two stages. Carbonization was carried out by step heating (mode 1) (Figure 1, curve *1*),[23] followed by reimpregnation of the sample with phthalonitrile resin and heating up to 1800 °C using the following program: 20 → 1800 °C at 6 °C min^{-1}, dwell at 1800 °C for 1 h.

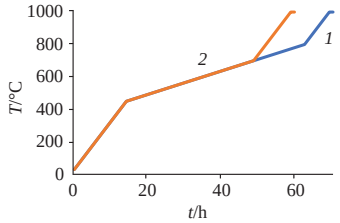

Figure 1 Carbonization modes.

Carbonization according to the described mode 1 takes over 63 h; therefore, an improvement of the material processability can be achieved by reducing this time. To define the temperature interval where the heating rate can be raised, sets of samples were subjected to 'partial carbonization': the samples were placed in an oven and heated according to mode 1, with the program interrupted at temperatures in the range 450–1000 °C (temperature interval of the phthalonitrile mass loss)[23] with a 50 °C step. After reaching the target interruption temperature and dwell for 1 h the samples were finally cooled to room temperature. Thus, the first sample set was heated from 20 °C to 450 °C at a heating rate of 1°C min^{-1} and held at 450 °C for 1 h, the second sample set from 20 °C to 450 °C (1°C min^{-1}), from 450 °C to 500 °C (0.12 °C min^{-1}) and held at 500 °C for 1 h, *etc*.

CFRP sample sets manufactured with two different phthalonitrile compositions (PN-1 and PN-2) were used. Such parameters as mass changes, shrinkages, densities, and interlaminar shear strengths (ILSS) were evaluated (see details in Online Supplementary Materials) for every set of samples (Figure 2). Changes in the controlled parameters were estimated

to evaluate the contribution of each temperature interval to carbonization. Mass losses were used to estimate carbonization conversion based on the carbon content in each sample. As much as noncarbon atoms are expected to be eliminated from the sample during the carbonization process, it is important to compare the actual mass loss with the mass content of all noncarbon atoms to better understand the carbonization mechanism and conversion. The ILSS values indicate indirectly the fiber–matrix interface strength and generally describe it and quality of the resulting materials. Shrinkage and density changes take place due to the densification process. It occurs owing to the formation of new carbon–carbon bonds along with the removal of noncarbon atoms. Shrinkage is also a crucial process which should be studied quantitatively to adjust the fabrication process, *e.g.*, simulating part shape changes after fabrication to make proper tooling. The density increment also shows indirectly the grade of composite matrix carbonization. However, we assume that at the high heating rate, due to the fast decomposition of the matrix, the escaping gases originating from the removed noncarbon gases cause the formation of voids and cracks instead of an open microporosity canal system evolving at the lower heating rate.

Due to the lower mass loss values obtained for PN-1, along with the proximity of other parameters (Figure 2), this CFRP was selected for further study. The density and shrinkage [Figures 2(*a*) and 2(*c*), respectively] growth occurs mainly in the interval of 450–700 °C. Further low-rate heating does not look necessary as no significant changes in the sample geometry take place. Therefore, we decided to shorten the low-rate heating step from 450–800 °C (sample 1) to 450–700 °C (sample 2) and to carry out the heating from 700 to 1000 °C with a rate of 0.5 °C min^{-1} (Figure 1, curve *2*). In a previous work, it was shown that further increase of the heating rate from 450 to 700 °C results in the higher rate of formation of the emitting gases which causes material cracking.[23] Despite the formation of the matrix lattice which happens mostly at temperatures between 450 and 700 °C, the mass loss values [Figure 2 (*d*)] continue to grow up to 1000 °C. Hence, gas evolution takes place at temperatures up to 1000 °C and further rate increase when heating from 700 to 1000 °C can lead to an adverse result as well. Thus, sample 2 carbonization mode is as follows: 20 → 450 °C, 1 °C min^{-1}, 450 → 700 °C, 0.12 °C min^{-1}, 700 → 1000 °C, 0.5 °C min^{-1}, dwell at 1000 °C, 1 h. Comparison of data received for samples 1 and 2 revealed minor differences in mass loss, shrinkage, ILSS, density and porosity (Table 1). The main advantage of sample 2 mode is a significant time decrease (52 h compared with 63 h in sample 1 mode) whilst the properties of the materials remain almost the same. Thus, sample

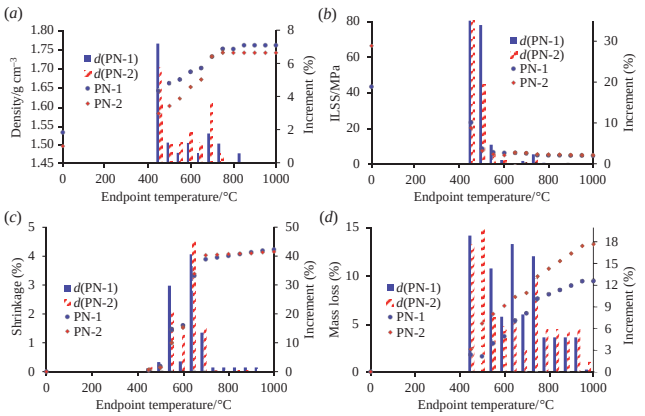

Figure 2 Controlled parameter changes during incomplete carbonization. The dots (PN-1 and PN-2) represent the absolute values of the measured parameters after each step. The bars [*d*(PN-1) and *d*(PN-2)] represent the relative increment in the value per step.

Table 1 Characteristics of samples 1 and 2.

Sample	Mass loss (%)	Shrinkage (%)	ILSS/ MPa	Density/ g cm^{-3}	Porosity (%)	Open porosity volume/ ml g^{-1}
Sample 1	11.68	2.96	7.2	1.71	21.94	0.08
Sample 2	11.49	2.90	7.6	1.72	22.19	0.08
Diff. (%)	–1.63	–2.03	5.5	0.78	1.1	0

2 mode is preferable for carbonization of CFRP with PN matrix. The heating rate in the temperature range from 20 to 450 °C can be further increased owing to the stable structure ($T_{5\%}$ > 450 °C) of phthalonitriles. However, it should be noted that large furnaces could overheat the sample by inertia after dropping the heating rate at 450 °C, which can be crucial to the sample properties. On the other hand, a heating rate in the 700 → 1000 °C range cannot be increased because gas evolution still takes place at these temperatures so that extensive cracking happens in bulk samples.

The mercury intrusion porosimetry which was used to measure the sample porosities allows one to evaluate only meso- and macroporosity. As long as the vacuum infusion process enables the pressure gradient of only 1 bar, microporosity cannot be impregnated under such conditions. Hence, the mercury intrusion porosimetry data is sufficient to estimate the required resin volume. However, mercury intrusion porosimetry does not allow one to estimate the closed porosity within samples. The closed porosity is a defect that originates from the initial carbonization process. Therefore, the only way to decrease the closed to opened porosity ratio is to increase the heating rate to form the wider channels of the evolving gases. On the other hand, excessive heating rate can result in the larger cracks, which significantly reduces the sample mechanical characteristics. Thus, a balanced heating rate is required.

The C/C samples obtained after first carbonization were reimpregnated with a phthalonitrile resin PNT (see details in Online Supplementary Materials). After the second infusion process, the C/C sample mass increased by 9.6%. The filled porosity ratio (FPR) can be calculated using the following equation:

$$\mathrm{FPR} = 100\% \frac{(m_2 - m_1)/\rho(\mathrm{PNT})}{\mathrm{OPV}\ m_1} = 100\% \frac{m_2/m_1 - 1}{\mathrm{OPV}\ \rho(\mathrm{PNT})}, \quad (1)$$

where m_1 – composite mass before second infusion; m_2 – composite mass after second infusion; ρ(PNT) – density of the postcured resin PNT; OPV – opened porosity volume of the composite before second infusion. Considering the PNT resin density as 1.3558 g cm^{-3}, we estimated that 88.5% of the initial porosity was filled.

Two different sample sets of C/C composites after one infusion/carbonization cycle were prepared for graphitization: the first was used ‘as is’ after carbonization (sample 3), the second was impregnated with PNT resin after carbonization and cured according to the temperature program (see details in Online Supplementary Materials) (sample 4). Graphitization stage for both samples was carried out according to the following mode: heating from 20 to 1800 °C, 6 °C min^{-1}, dwell at 1800 °C, 1 h. The carbon lattice is formed mainly during the initial carbonization. The main reason for sample cracking is gas evolution, produced mostly from noncarbon atoms. The quantity of the noncarbon atoms from carbonized matrix and the pores filling resin is too low to break the composite structure. Therefore, the low-rate heating is unnecessary.

SEM images of the obtained C/C composites are depicted in Figure 3. Mercury intrusion porosimetry data for these samples are given in Table 2. Average pore diameter decreases after the graphitization for a reimpregnated C/C composite and increases

Table 2 C/C composite properties after one and two impregnation–carbonization cycles.

Sample	Density/g cm^{-3}	ILSS/MPa	Compression strength/MPa	Coefficient of friction	Average pore diameter/μm	Total pore area/m^2 g^{-1}
Carbonization (sample 2)	1.71	7.1	107.6	0.31–0.33	14	0.024
Carbonization + impregnation + graphitization (sample 4)	1.73	14.1	139.8	0.32–0.34	7.1 (sample 3 – 18)	0.106 (sample 3 – 0.132)
Carbonization + impregnation + carbonization (sample 5)	1.71	7.9	—	—	—	—
Literature data	1.77[25] 1.58[26] 1.5[27] 1.67– 1.70[29]	11.4[25] 12.4– 14.1[29]	111[25] 108[26] 150–200[28]	0.1–0.47[30]	—	—

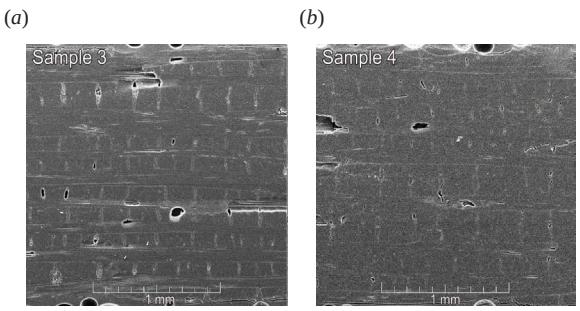

Figure 3 SEM images of C/C composites after two carbonization cycles: (*a*) carbonized sample, used 'as is' after carbonization; (*b*) carbonized sample, reimpregnated with PN resin after carbonization and curing process according to the graphitization temperature program.

for a non-reimpregnated sample. It shows that graphitization at 1800 °C causes a further structure transformation and increase in pores size. Small pores can be filled during the further chemical vapor infiltration process. Wider pores remain as a defect since they cannot be filled completely. That can be explained by the formation of the evolved gases from the residual noncarbon atoms and noncarbon atoms from the newly impregnated resin. Mass loss for samples 1 and 2 is 4.11 and 8.99%, respectively. The higher value of the mass loss for the sample 4 is due to the higher content of noncarbon atoms from the impregnated resin. For samples 3 and 4 composites shrinkage during graphitization process does not exceed 1% along the *z* axis and is absent along the *x* and *y* axes.

A thermoset (see details in Online Supplementary Materials) was obtained from the neat PNT resin and heated according to the same procedure as sample 1. Resulting materials were studied *via* X-ray crystallography analysis to estimate the carbon matrix morphology at each step of fabrication (Figure 4).

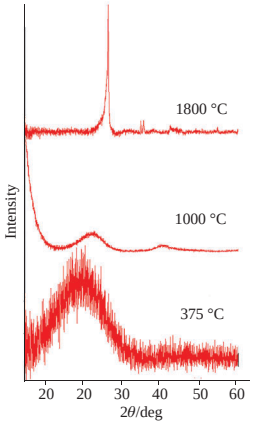

Figure 4 X-ray crystallography results for the thermoset (375 °C) and the carbonized thermosets (one cycle – 1000 °C, two cycles – 1800 °C).

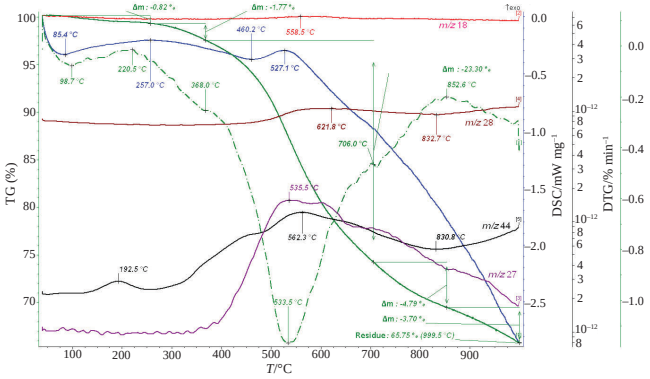

Figure 5 Cured phthalonitrile thermoset pyrolysis TGA-MS data: *m*/*z* = 18 corresponds to H_2O, *m*/*z* = 27 – to HCN, *m*/*z* = 28 – to N_2, *m*/*z* = 44 – to CO_2.

Predictably, the initial thermoset was amorphous. The crystalline phase content grows with an increase in treatment temperature and a graphite-like lattice appears after treatment at 1800 °C. Elemental analysis reveals an increase in carbon mass content and decrease in hydrogen mass content and nitrogen elimination (as N_2 and HCN, see Figure 5) after treatment at 1800 °C (Table 3). It is also seen that the sum of the element contents is not equal to 100%, which may indicate the presence of oxygen due to partial oxidation of the samples or residual phosphorus. The data clarifies the nature of the substances accountable for the mass loss. Since the noncarbon atom content decreases, the theoretical residual sample mass is limited at the lower margin by the mass of the carbon atoms for a carbon-only matrix at the end of the treatment. Therefore, the phthalonitrile graphitization treatment at 1800 °C allows one to obtain materials almost entirely composed of carbon atoms with a relatively low mass loss throughout the carbonization process.

The properties of C/C composites produced in one and two impregnation–carbonization cycles are shown in Table 2. Sample 4 was obtained following the graphitization treatment (1800 °C) during the second cycle, as described above. Sample 5 was derived from the same reimpregnated preform as sample 4, but instead of graphitization it was carbonized by the sample 2 carbonization mode. It is notable that ILSS significantly increases after the second cycle with carbonization (sample 5) and graphitization (sample 4). The ILSS indirectly shows the fiber–matrix interface improvement. Despite the

Table 3 Elemental analysis data for the thermoset (375 °C) and the carbonized thermosets (one cycle – 1000 °C, two cycles – 1800 °C).

Treatment temperature/°C	C (%)	H (%)	N (%)
375	69.94	4.18	12.96
1000	91.58	1.13	1.09
1800	96.13	1.38	0.00

porosity value increase, the mechanical performance and carbon content grow significantly. The commercial samples are usually manufactured through the chemical vapor infiltration or impregnation with phenolic resin or pitch. However, the former approach requires a specific needled felt preform composites, which can be expensive and limits their applications. Utilization of phthalonitriles provides not only better processability, but superior characteristics compared with the chemical vapor infiltration-made materials.[25] Phenolic resins, on the other hand, show low density after the first carbonization[26,27] therefore, several reimpregnation–carbonizations are needed. Thus, it takes more time to provide the mechanical characteristics comparable to the C/C composites derived from phthalonitrile-matrix CFRP.[28] Pitch impregnation allows one to obtain materials with higher density and interlaminar shear strength values.[29] However, pitch has relatively poor processability compared to phthalonitriles. Therefore, the use of phthalonitrile resins enables to manufacture C/C composite samples possessing competitive properties after only two-step processing.

In conclusion, C/C composites obtained in this work showed promising properties after the shorter fabrication procedure, including carbonization of CFRP at 1000 °C followed by reimpregnation with phthalonitrile resin and graphitization of the produced material at 1800 °C. The time of the initial CFRP carbonization process was reduced from 63 to 52 h. Phthalonitrile resin high carbon yield provides high C/C material manufacturing rate. Double-cycled composites can meet the technical requirements for heavy vehicle brakes[30] and construction applications. Thus, phthalonitrile resins can be used in the carbon–carbon composites manufacturing owing to the easy processing and good performance.

This work was carried out in the framework of the state assignment of the Department of Chemistry of the M. V. Lomonosov Moscow State University (project no. AAAA-A21-121011590086-0).

This research was performed according to the Development program of the Interdisciplinary Scientific and Educational School of Lomonosov Moscow State University ‘The future of the planet and global environmental change’.

Online Supplementary Materials

Supplementary data associated with this article can be found in the online version at doi: 10.1016/j.mencom.2022.05.011.

References

1 L. M. Manocha, *Sadhana*, 2003, **28**, 349.
2 G. Yuan, X. Li, Z. Dong, X. Xiong, B. Rand, Z. Cui, Y. Cong, J. Zhang, Y. Li, Z. Zhang and J. Wang, *Carbon*, 2014, **68**, 413.
3 S.-J. Park and M.-K. Seo, *Interface Science and Composites*, Elsevier, Amsterdam, 2011, vol. 18, pp. 501–629.
4 J. D. Buckley and D. D. Edie, *Carbon-Carbon Materials and Composites*, Noyes Publications, Park Ridge, NJ, 1993.
5 R. M. Mohanty, *Def. Sci. J.*, 2013, **63**, 531.
6 G.-Y. Chen, Z. Li, P. Xiao, X. Ouyang, W.-J. Ma, P.-T. Li, J.-W. Li and Y. Li, *Trans. Nonferrous Met. Soc. China*, 2019, **29**, 123.
7 R. Taylor, S. B. Venkata Siva and P. S. Rama Sreekanth, in *Comprehensive Composite Materials II*, 2nd edn., Elsiever, Amsterdam, 2017, vol. 5, pp. 339–378.
8 P. Xiao, Z. Li, Z. Zhu and X. J. Xiong, *Mater. Sci. Technol.*, 2010, **26**, 283.
9 E. Fitzer and L. M. Manocha, *Carbon Reinforcements and Carbon/Carbon Composites*, Springer, Berlin, 1998.
10 K. M. Chioujones, W. Ho, B. Fathollahi, P. C. Chau, P. G. Wapner and W. P. Hoffman, *Carbon*, 2006, **44**, 284.
11 B. Fathollahi, P. C. Chau and J. L. White, *Carbon*, 2005, **43**, 125.
12 B. Fathollahi, M. Mauldin, P. C. Chau, P. G. Wapner and W. P. Hoffman, *Carbon*, 2006, **44**, 854.
13 L. M. Manocha, in *Handbook of Advanced Ceramics*, 2nd edn., ed. S. Somiya, Academic Press, 2013, pp. 171–198.
14 T.-H. Ko, W.-S. Kuo and Y.-R. Lu, *Polym. Compos.*, 2000, **21**, 96.
15 S. J. Mitchell, R. S. Pickering and C. R. Thomas, *J. Appl. Polym. Sci.*, 1970, **14**, 175.
16 B. A. Bulgakov, O. S. Morozov, I. A. Timoshkin, A. V. Babkin and A. V. Kepman, *Polym. Sci., Ser. C*, 2021, **63**, 64.
17 B. A. Bulgakov, A. V. Sulimov, A. V. Babkin, D. V. Afanasiev, A. V. Solopchenko, E. S. Afanaseva, A. V. Kepman and V. V. Avdeev, *Mendeleev Commun.*, 2017, **27**, 257.
18 V. E. Terekhov, V. V. Aleshkevich, E. S. Afanaseva, S. S. Nechausov, A. V. Babkin, B. A. Bulgakov, A. V. Kepman and V. V. Avdeev, *React. Funct. Polym.*, 2019, **139**, 34.
19 B. A. Bulgakov, K. S. Belsky, S. S. Nechausov, E. S. Afanaseva, A. V. Babkin, A. V. Kepman and V. V. Avdeev, *Mendeleev Commun.*, 2018, **28**, 44.
20 B. A. Bulgakov, A. V. Sulimov, A. V. Babkin, I. A. Timoshkin, A. V. Solopchenko, A. V. Kepman and V. V. Avdeev, *J. Compos. Mater.*, 2017, **51**, 4157.
21 V. E. Terekhov, A. A. Bogolyubov, O. S. Morozov, E. S. Afanaseva, B. A. Bulgakov, A. V. Babkin, A. V. Kepman and V. V. Avdeev, *Mendeleev Commun.*, 2020, **30**, 796.
22 M. V. Yakovlev, O. S. Morozov, E. S. Afanaseva, B. A. Bulgakov, A. V. Babkin and A. V. Kepman, *React. Funct. Polym.*, 2020, **146**, 104409.
23 V. V. Aleshkevich, A. V. Babkin and V. V. Avdeev, *IOP Conf. Ser.: Mater. Sci. Eng.*, 2019, **683**, 012023.
24 S. B. Sastri, J. P. Armistead and T. M. Keller, *Carbon*, 1993, **31**, 617.
25 J. Jia, J. Ju, S. Liu and G. Ji, *Ceram. Int.*, 2021, **47**, 24262.
26 M. S. Inoue, *Patent US5071700A*, 1991.
27 C. Scarponi, in *Advanced Composite Materials for Aerospace Engineering*, 1st edn., eds. S. Rana and R. Fangueiro, Elsevier, Amsterdam, 2016, pp. 385–412.
28 A. P. Mouritz, *Introduction to Aerospace Materials*, Woodhead Publishing Ltd., Oxford, 2012, pp. 394–410.
29 P. D. Matzinos, J. W. Patrick and A. Walker, *Carbon*, 1996, **34**, 639.
30 T. J. Yager, *1st International Meeting on Aircraft Performance Contaminated Runways (IMAPCR ’96)*, Montreal, Quebec, 1996, document ID 19970000907.

Received: 15th September 2021; Com. 21/6693